Trans Indian Inst Met (2021) 74(7):1623–1637
https://doi.org/10.1007/s12666-021-02265-y

ORIGINAL ARTICLE

Mechanical and Microstructural Characteristics of Gas Tungsten Arc Welded Similar and Dissimilar Joints of SS-316 L and Hastelloy C276

Sreenivasulu Bezawada[1] · Rajyalakshmi G[1]

Received: 14 September 2020 / Accepted: 18 April 2021 / Published online: 27 April 2021

Abstract Hastelloy C-276 nickel alloy is widely preferred for nuclear power plant applications where steam generators operate at 600 °C. However, stainless steels are still used for tubes in steam gas reformers which necessitates welds between dissimilar materials. In this study, hastelloy C-276 and SS 316 L alloys were joined using GTAW process. The welding parameters of GTAW were optimized to minimize the defects in samples of similar (SS 316 L-SS 316 L, HAS C-276-HAS C-276), and dissimilar (HAS C-276-SS 316 L) joints. SEM/EDS results confirm the presence of columnar dendritic and cellular structure in fusion zone for dissimilar weldments (HAS C-276-SS 316 L). EDS results also revealed the presence of larger amount of Mo, W and lower amount of Ni in the subgrain boundary as compared to the subgrain body. Compared to the similar (HAS C-276- Has C-276) and dissimilar (HAS C-276-SS 316 L) welded joints FZs, the enrichment of Mo is lesser in SS 316 L-SS 316 L similar welded joints. Higher UTS was obtained for dissimilar (HAS C-276-SS 316 L) GTAW joints 780 MPa compared to the similar welded joints of SS316 (552 MPa) and HAS C-276 (740 MPa). The average microhardness for the dissimilar SS 316 L and HAS C-276 is 220 Hv, which is higher compared to the similar welded joints, SS 316 L and HAS C-276, i.e., 190 Hv and 210 Hv, respectively. This study shows that GTAW process is suitable to fabricate sound weld joints of similar (SS 316 L- SS 316 L, HAS C-276-HAS C-276), and dissimilar (HAS C-276-SS 316 L) alloys which are useful for the nuclear power plant boilers.

✉ Rajyalakshmi G
rajyalakshmi@vit.ac.in

[1] School of Mechanical Engineering, Vellore Institute of Technology, Vellore 632 014 Tamilnadu, India

Keywords SS 316 L austenitic stainless steel · Hastelloy C-276 · Continuous current gas tungsten arc welding · Fusion zone · Tungsten arc welding

1 Introduction

Joining of dissimilar materials using fusion welding techniques is extensively studied to reduce the material cost or service requirement of the welded components [1]. Material which has combination of both good mechanical properties and superior corrosion resistance are generally preferred for equipment subjected to heavy mechanical loads in severe environments like those in nuclear power plants. Among many nickel-based superalloys, the Hastelloy C-276 are considered to be best in the producing these combinations of properties. Hence, C-276 is widely preferred for nuclear power plant applications where steam generators operating temperature could be over 600 °C [2, 3]. However, because of their high cost, alternate materials for the Haste alloy C-276 are still employed wherever possible. Stainless steel (SS) may be a one of the alternates for Hastelloy C-276, because of its higher erosion resistance and considerable mechanical properties [3]. However, the examination on the dissimilar joints of nickel-based superalloys and SS has been carried out and archived. But investigate information accessible on peculiar combination of C-276 and SS316 L have not been considered widely. Additionally, in super-critical water gas (SCWG) reactors, which are used to convert biomass into gaseous fuels, the main reactor shell is subjected to harsh working conditions like high temperatures, pressures, and corrosive chemical environment. The header to nozzle joint

Table 1 Base material properties

	Mo	Cr	W	Co	Mn	Fe	Si	v	Ti	C	P	S	Ni
Hastelloy C-276	16.36	15.83	3.45	0.05	0.41	6.06	0.02	0.17	–	0.005	–	–	Bal
SS 316L	2–3	16–18	–	–	2.0	–	0.75	–	–	0.03	0.045	0.03	10–14

Table 2 Mechanical properties of base metal [11&7]

Base materials	Yield strength [MPa]	Ultimate tensile strength [MPa]	Elongation [%]	Reduction in cross-sectional area [%]	Notch tensile strength [MPa]	Notch strength ratio
Hastelloy C-276	542.5	748	47	46	829.5	1.10
SS 316L	429.5	564	44	46.5	663	1.17

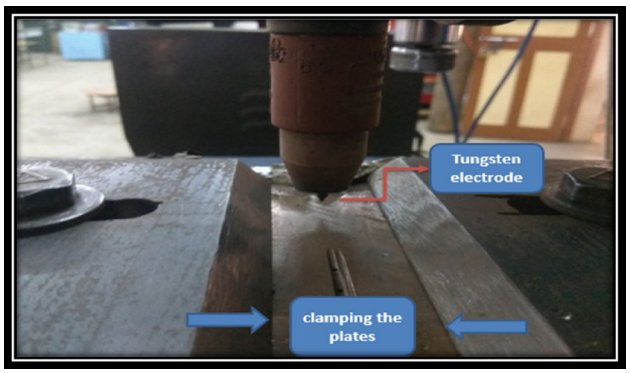

Fig. 1 Photograph of clamping the plates

or the shell to channel joint in these reactors would need a dissimilar weld joint [4, 5]. Hence, it is worthwhile to study the weld joint interface of two dissimilar materials like Hastelloy C-276 and SS 316L made by using different welding processes. The results of such investigation will be useful in many high-temperature applications.

There are many more complication in joining dissimilar materials as compared to joining similar materials. One important issue in joining of two dissimilar materials arises from their different chemical properties [1, 3, 4]. Mostly, the joining of dissimilar weld metals is fabricated using different arc welding processes such as shielded metal arc welding (SMAW), gas metal arc welding (GMAW) and gas tungsten arc welding (GTAW) [5, 6]. Among these different welding techniques GTAW is especially preferred to join dissimilar materials [7, 8], since it facilitates the joining of materials with non-consumable electrode, which is both cost-effective and time saving.

Dokme et al. 2018 [9] joined dissimilar metal Inconel 625 and AISI 316L using the continuous current gas tungsten arc welding (CCGTAW) and pulsed current gas tungsten arc welding (PCGTAW) processes using different filler materials like ERNiCr-3, TIG 316L and twisted (ERNiCr-3 and TIG 316L). Authors reported that the PCGTAW welded samples with twisted filler produced sound mechanical property. Earlier, Sharma et al. 2017 [10] joined Hastelloy and AISI 321 austenitic stainless steel using ERNiCrMo-4 filler by GTAW and PCGTAW. The authors concluded that compared to CCGTAW joints PCGTAW joints resulted in sharp weld bead, fine grains, less elemental segregation, and higher ultimate tensile strength. Pandit et al. 2014 [11] studied joining of dissimilar weldments of Monel 400 and Hastelloy C276 by GTAW process with ERNiCrMo-3 filler wire. The authors reported that the quality of the weld zone is higher as compared to the parent metals. Sharma et al. 2018 [12] reported that dissimilar joints of superalloy C-276/stabilized grade 321 using PCGTAW process microstructure shows columnar and cellular dendritic structure because of higher heat input in the weldments and revealed that the lower heat input weldments show equiaxed and cellular dendritic structure.. Ramesh Kumar et al. 2011 [13] welded dissimilar SS 304 and 316 using TIG, laser, and electron beam welding, and authors have characterized the welded joints using NDT techniques. Mishra et al. 2014 [14] studied tensile strength of MIG and TIG welded dissimilar joints of mild steel and stainless steel. The tensile results revealed that TIG-welded dissimilar joints have sound mechanical properties as compared to MIG welded joints. Taraphdar et al. 2020 [15] studied intergranular stress corrosion cracking of AISI 304L stainless steel and analyzed the temperature history of two different groove designs such as conventional and narrow groove. Pandey et al. 2018 [16] studied microstructure evolution in P91 steel and their weldments. Author concluded that the initial microstructure plays an important role in deciding the mechanical properties of P91 steel. Sirohi et al. 2020 [17] investigated the microstructure and mechanical behavior of the dissimilar welded joint of martensitic A 335-grade P91 steel and high alloy ferritic austenitic A 182 F69 steel produced by the GTAW process. Author concluded that the tensile strength of the dissimilar welded joint was high for

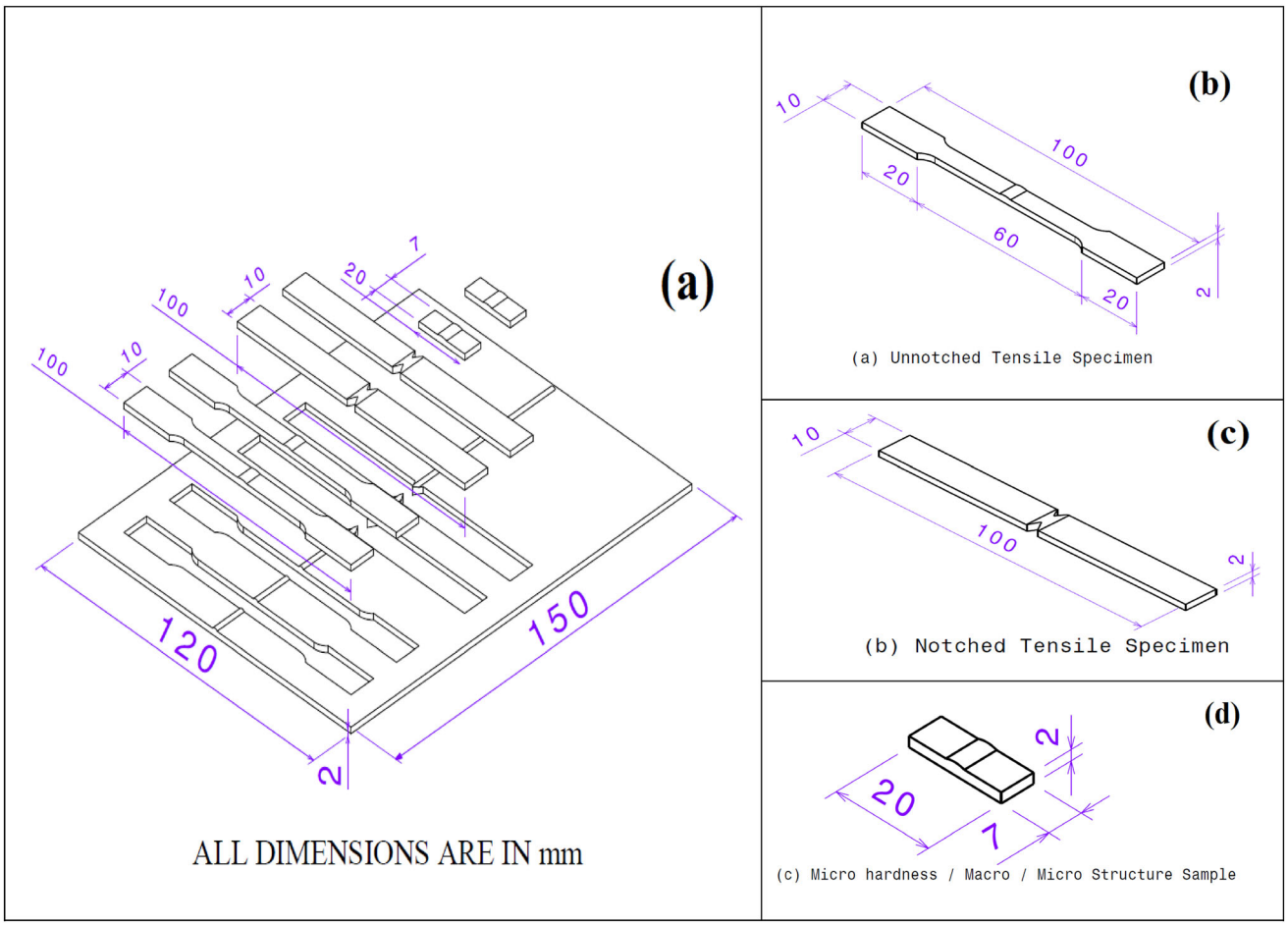

Fig. 2 Dimensions of specimens (**a**) Tensile specimen (unnotched) (**b**) Tensile specimen (notched), and (**c**) Microhardness / Macro- and microstructure sample (**d**)

Table 3 Level of CCGTAW process parameters

Weld technique	Process parameters	Hastelloy C-276 – Hastelloy C-276	SS 316L-SS 316L	Hastelloy C-276-SS316
CCGTAW	Mean Current (A)	65	85	75
	Weld speed (mm/s)	70	70	70
	Gas flow rate (1/min)	16	16	16
	Type of shielding gas	Pure argon (99.99%)	Pure argon (99.99%)	Pure argon (99.99%)

as-welded condition and reduced after the PWHT. Pandey et al. 2017 [18] investigated the dissimilar weld joint of P91 and P92 steel joint were made using the autogenous TIG welding with single pass, double side pass and multi-pass GTA welding with filler wire. Author concluded that the peak hardness and poor impact toughness were observed for autogenous TIG welds joint as compared to GTA welds.

From the extensive literature review, it was observed that no author has reported the joining of Hastelloy C276 Ni-base superalloy and austenitic stainless steel SS316L by using GTAW. Hence, in this investigation, an attempt has been made to fabricate dissimilar joints of Hastelloy C276 and austenitic stainless steel SS316L using GTAW. Moreover, the similar joints of C-276 and SS316L materials also fabricated using GTAW and studied to understand the variation in microstructure and mechanical property with dissimilar combination of these materials.

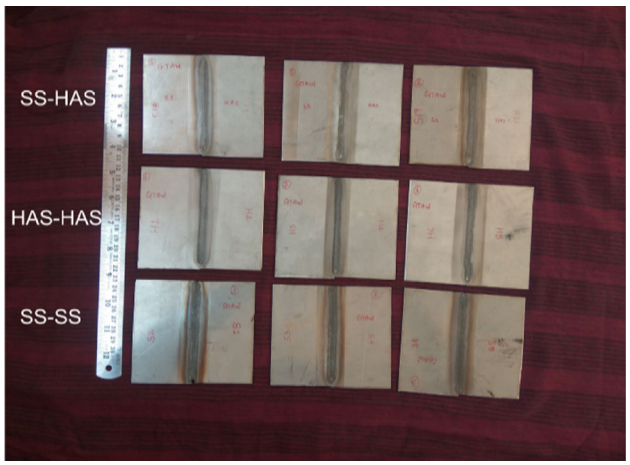

Fig.3 Photograph of all welded joints combinations

2 Experimental Work

Hastelloy C-276 and SS316L are used as the base metals, both having 2 mm plate thickness. Due to this small thickness, both similar and dissimilar weld joints are fabricated using non-consumable GTAW electrode. The Hastelloy C-276 and SS316 was cut to the required size (100 × 60 × 2 mm) by wire cut machine. The chemical composition and mechanical properties of the base metals used in this study are given in Tables 1 and 2, respectively.

The necessary care (fixtures were used) was taken avoid joint distortion during welding process. The plates were securely clamped by using suitable clamping arrangement for making the joint as shown in Fig. 1. The base metals and welded joints were polished as per the metallographic procedures to obtain clear images of the micro- and macrostructures.

For SS 316L similar joints, the etching solution used consisted of 5 ml HCl + 5 ml HNO_3 + 1 g Copper Chloride. For HAS C-276 similar joints, the etching solution consisted of 7.5 ml HCl + 2.5 ml HNO_3. Similarly, for HAS C-276 and SS 316 L dissimilar combinations, the etching solution consisted of 100 cc H_2O + 10 g CrO_3 at 5 V for 1 min.

The autonomous welding method was used to make the butt joints for this sheet as shown in Fig. 2a. The welded joints were produced using tungsten inert gas welding machine (Lincoln, USA) with 400 A capacity. Countable number of trials was performed. After analyzing the macroprofile, the required combination of parameters to make the full penetration is identified. The optimized welding parameters for GTAW by similar and dissimilar weld joints is listed in Table 3.

Figure 2a shows the specimen image that was used to fabricate GTAW for similar and dissimilar weld joints in autogenous welding mode. Figure 2b shows the unnotched tensile specimens. After the joints were made, the specimens were cut in the transverse direction to study the yield strength, ultimate tensile strength (UTS), percentage of elongation, percentage of reduction in cross-sectional area (CSA), and joint efficiency. Figure 2c shows the notched tensile specimen. The notched tensile strength and notched strength ratio of the similar and dissimilar joints were found by using notched tensile specimen. As per the ASTM E8M-04 standard the tensile samples were prepared. To find UTS, the tensile test was carried out using a 100 kN, electro-mechanical controlled universal testing machine.

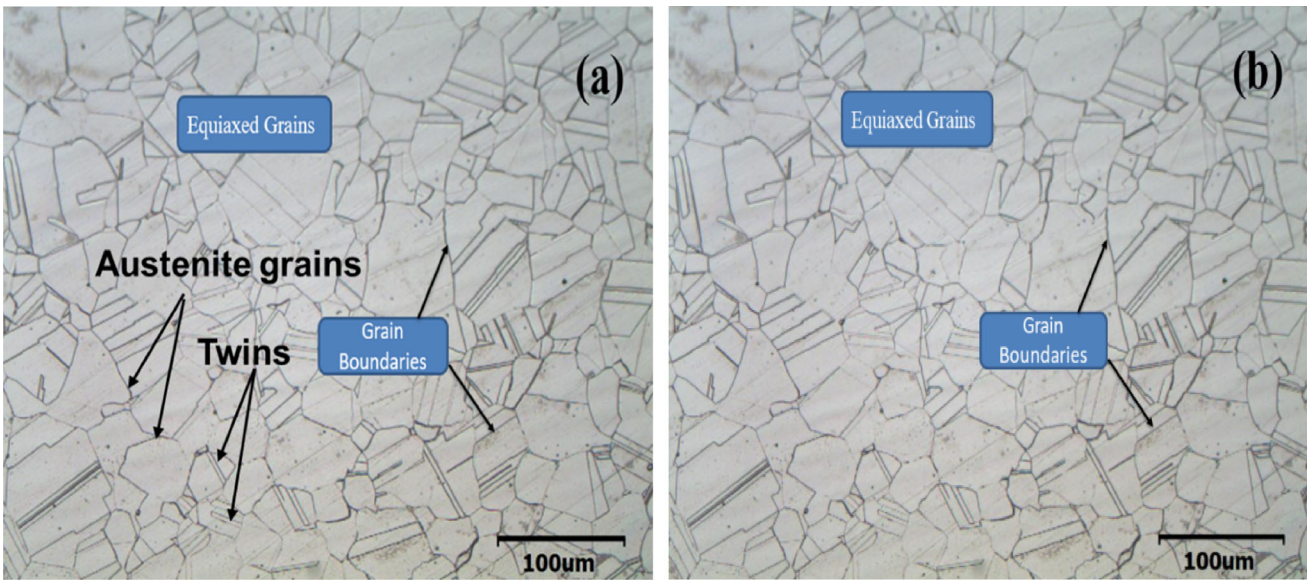

Fig. 4 Microstructure of SS 316 and Hastelloy C-276 in as received condition

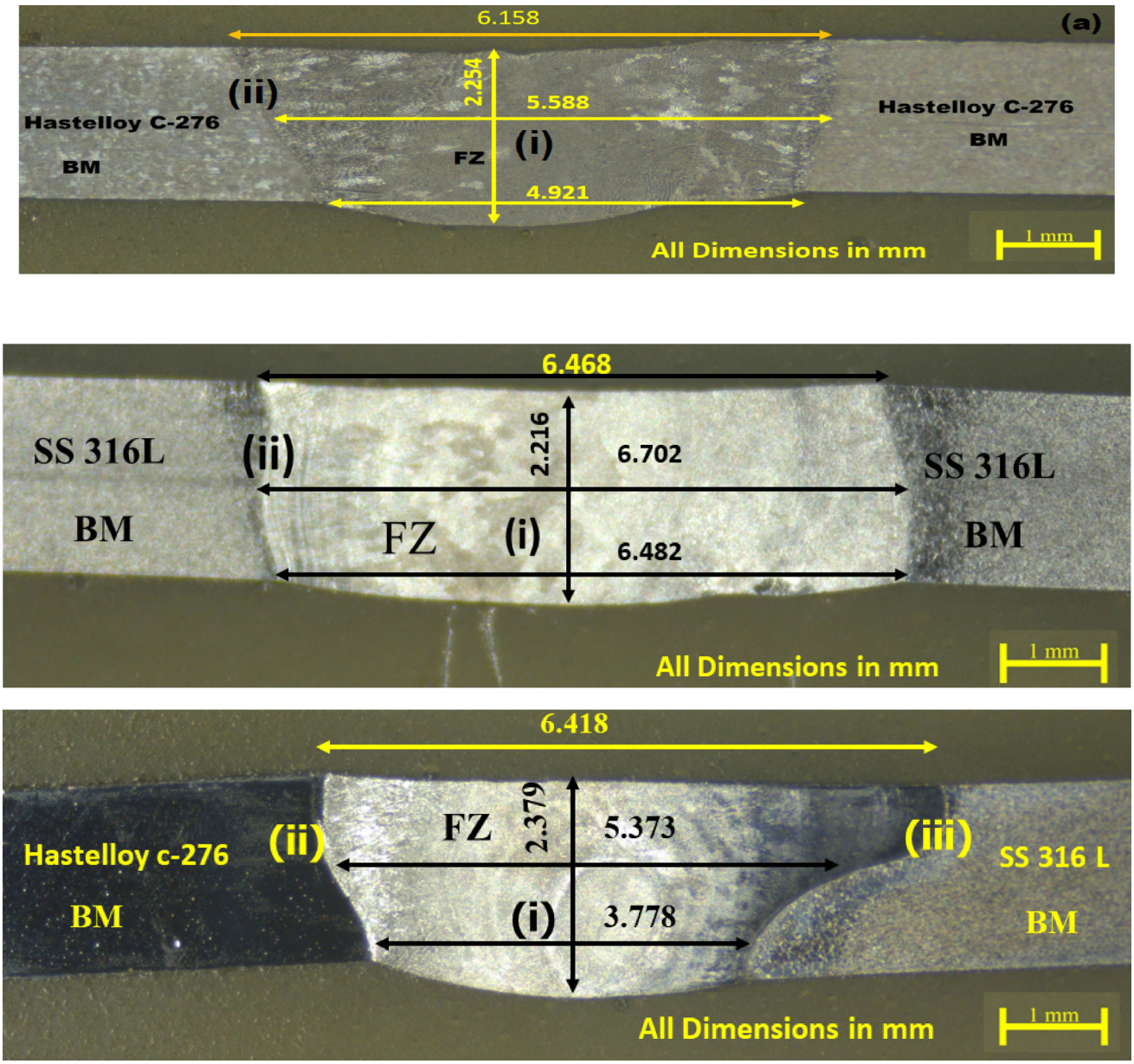

Fig.5 Macrostructure of weld joint produced: (**a**) Hastelloy C-276-Hastelloy C-276; (**b**) SS 316-SS 316; and (**c**) Hastelloy C-276-SS316

Along with tensile results, yield strength, UTS, and percentage of elongation were also recorded. The fractography of the failed area in the tensile samples was characterized using scanning electron microscope. Prior to the characterization, the samples were coated with commercial oil to avoid oxidation in the failed area [19]. Additionally, the specimens were also subjected to the ultrasonic cleaning with carbon tetrachloride and acetone to remove the impurities and moisture. The schematic representation of the macrohardness, macrostructure, and microstructure specimens is shown in Fig. 2d. The fabricated similar and dissimilar weldments using GTAW process are shown in Fig. 3. The microhardness test was performed in the sample across the joint with 0.05 kg load for 15 s on Vickers's microhardness testing machine.

3 Results and Discussion

3.1 Base Metal Investigation

Figure 4a shows the base metal microstructure of SS 316 L. SS 316L microstructure composed of fine grains with equiaxed grain structure. Also, an annealing twin was found in the austenitic matrix. Along and across the grain bodies and grain boundaries, the dotted inclusions and a

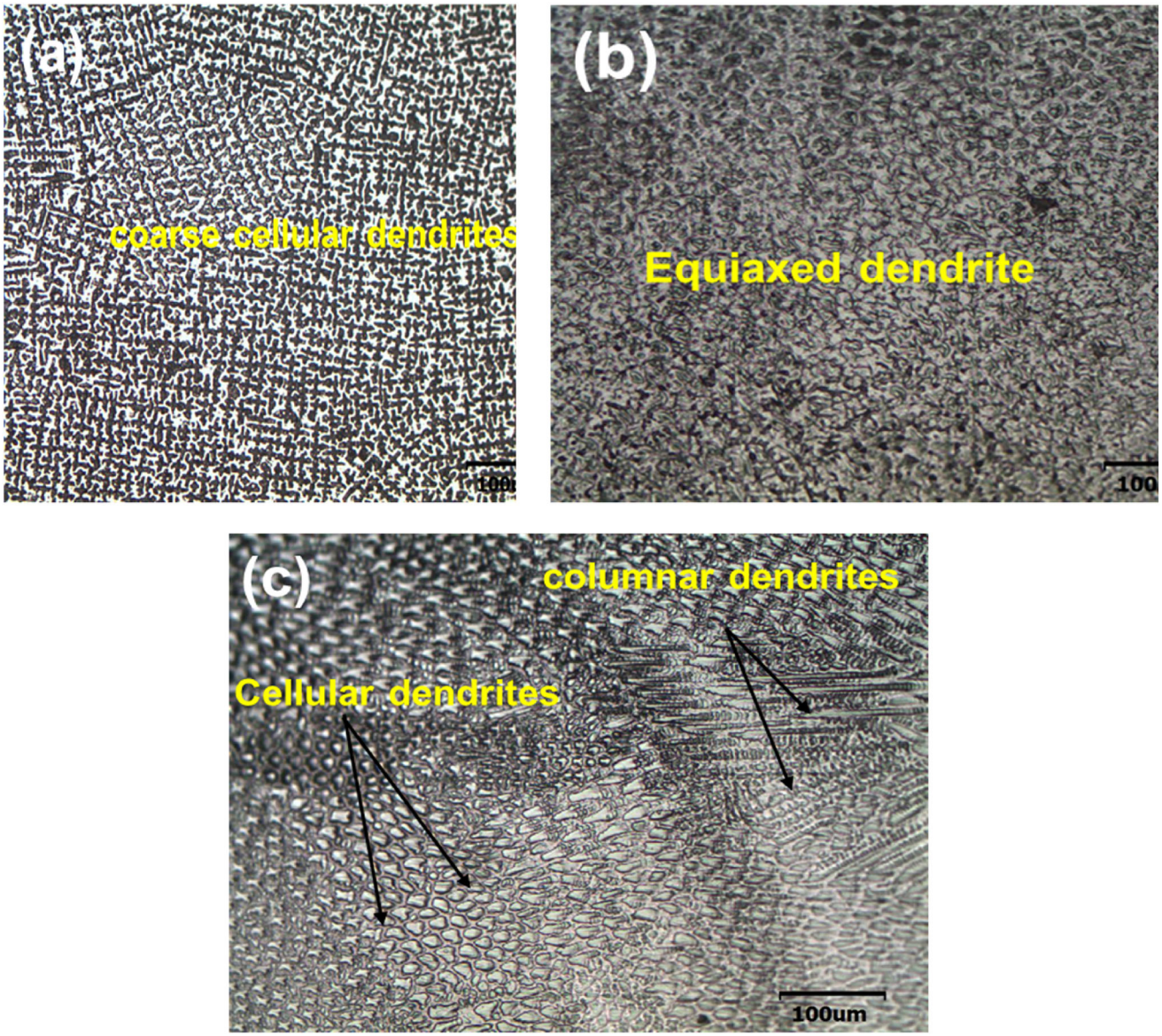

Fig.6 Fusion zone micrographs of the similar and dissimilar weldments for (**a**) HAS C-276-HAS C-276 (**b**) SS 316-SS316 (**c**) HAS C-276-SS316

small amount of delta ferrite was found [16]. Figure 4b shows the microstructure of Hastelloy C-276 BM, and it consists of fine-grain structures.

3.2 Macrostructural Investigation

Figure 5 shows the depth of penetration, width of bead, FZ and HAZ. The macrograph of GTAW was analyzed, and it was shown in Fig. 5a. It can be seen from these images that proper fusion has occurred during welding for both similar and dissimilar welded joints.

The process parameters used in this investigation was suitable to produce the weld samples with full penetration which is clearly evident from the macrographs. It is also noted from the images in Fig. 5 that the width at crown was higher for similar SS 316-SS 316 joints (6.468 mm) compared to those from similar HAS C-276-HAS C-276 (6.158) and dissimilar SS 316-HAS C-276 welded joints. Even though the difference in crown height between each similar and dissimilar welded appears to be small, its effect could still be significant in actual industrial applications.

3.3 Microstructural Examination

3.3.1 Fusion Zone Microstructures

Figure 6 shows the optical micrograph of FZ image of CCGTA weldments. For HAS C-276 similar joints, the

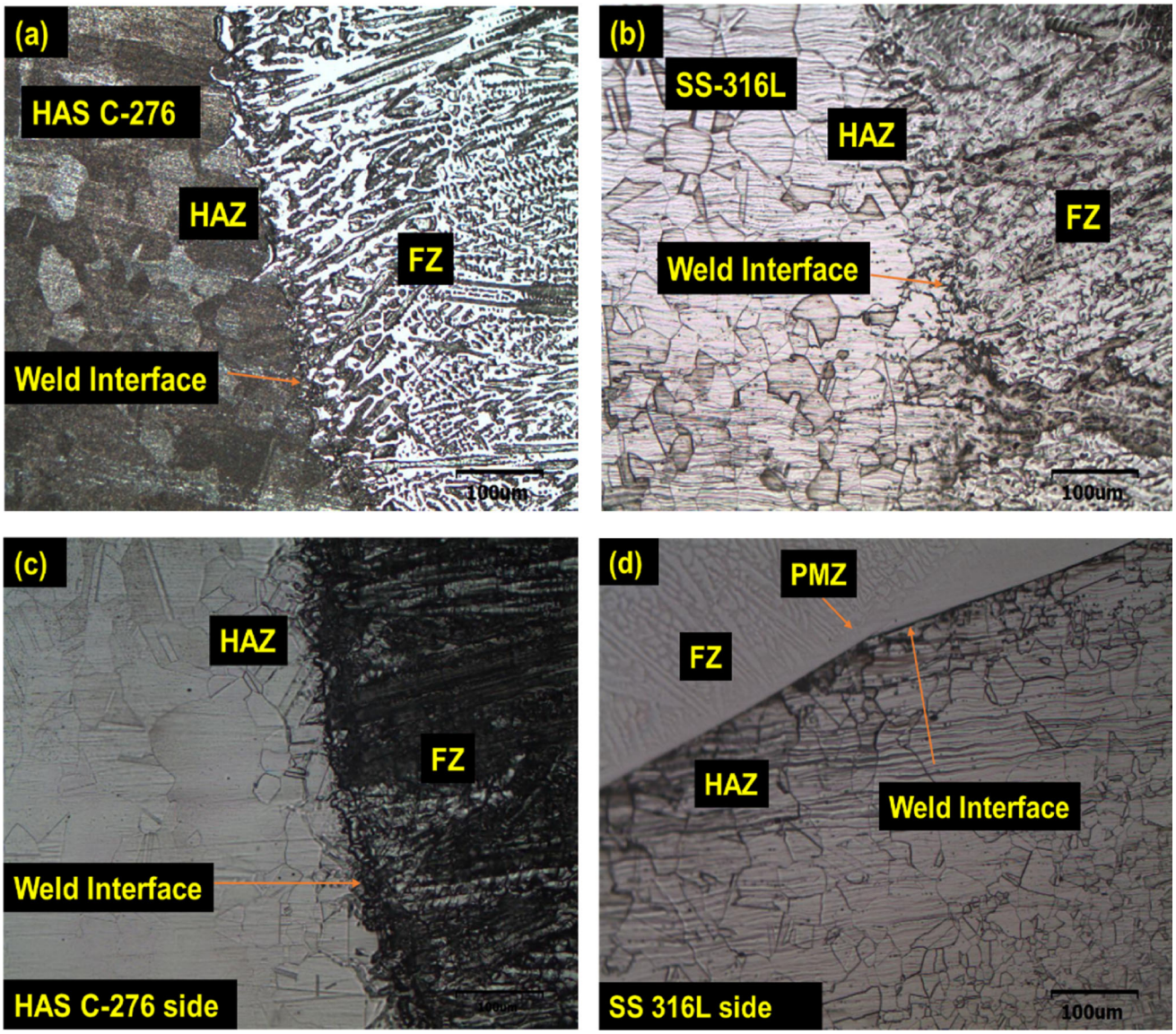

Fig.7 Microstructures of similar and dissimilar weldments welded with CCGTAW (**a**, **b**) Similar joint interface between weld, HAS C-276 and SS 316L, respectively. (**c**, **d**) Dissimilar joint interface between weld Hastelloy C-276 side, and SS 316L side, respectively

coarser cellular dendritic structure was clearly visible as shown in Fig. 6a (spot (i) in Fig. 5a). Equiaxed dendrites were present in the FZ microstructure for the similar SS 316L joints as shown in Fig. 6b (spot (i) in Fig. 5b). For the dissimilar SS 316L-HAS C-276 joints the FZ consists of both columnar dendritic and cellular dendrites as shown in Fig. 6c (spot (i) in Fig. 5c).

3.3.2 Interfacial Microstructures

Figure 7 shows the interfacial microstructure of weldments of similar and dissimilar joints of SS 316L and HAS C-276 weld metals using GTAW. Figure 7a–d shows microstructures of interfacial zone (IFZ) of GTAW weldments of similar HAS C-276 (Location ii in Fig. 5a), similar SS 316L (Location ii in Fig. 5b), dissimilar HAS C-276 side (Location ii in Fig. 5c), and SS 316L side (Location iii in Fig. 5c). Considerable grains coarsening arose in HAZ, as shown in Fig. 7a. Additionally, the secondary phases are also seen from the weld pass interface. Considering SS316 L in Fig. 7b, there is no accuracy in weld interface as compared to the HAS C-276 similar welded joints (See Fig. 7a). Due the higher input in GTAW process, the microstructures consist of partially melted zone (PMZ). PMZ occurs due to this higher heat input that associated with GTAW process that results in grain boundary melting and thickening (See Fig. 7d for SS 316L). Also, significant grain coarsening was obtained in the HAZ region. The higher heat input transferred from electrode to the weld metal during welding process may result in grain coarsening behavior. For HAS

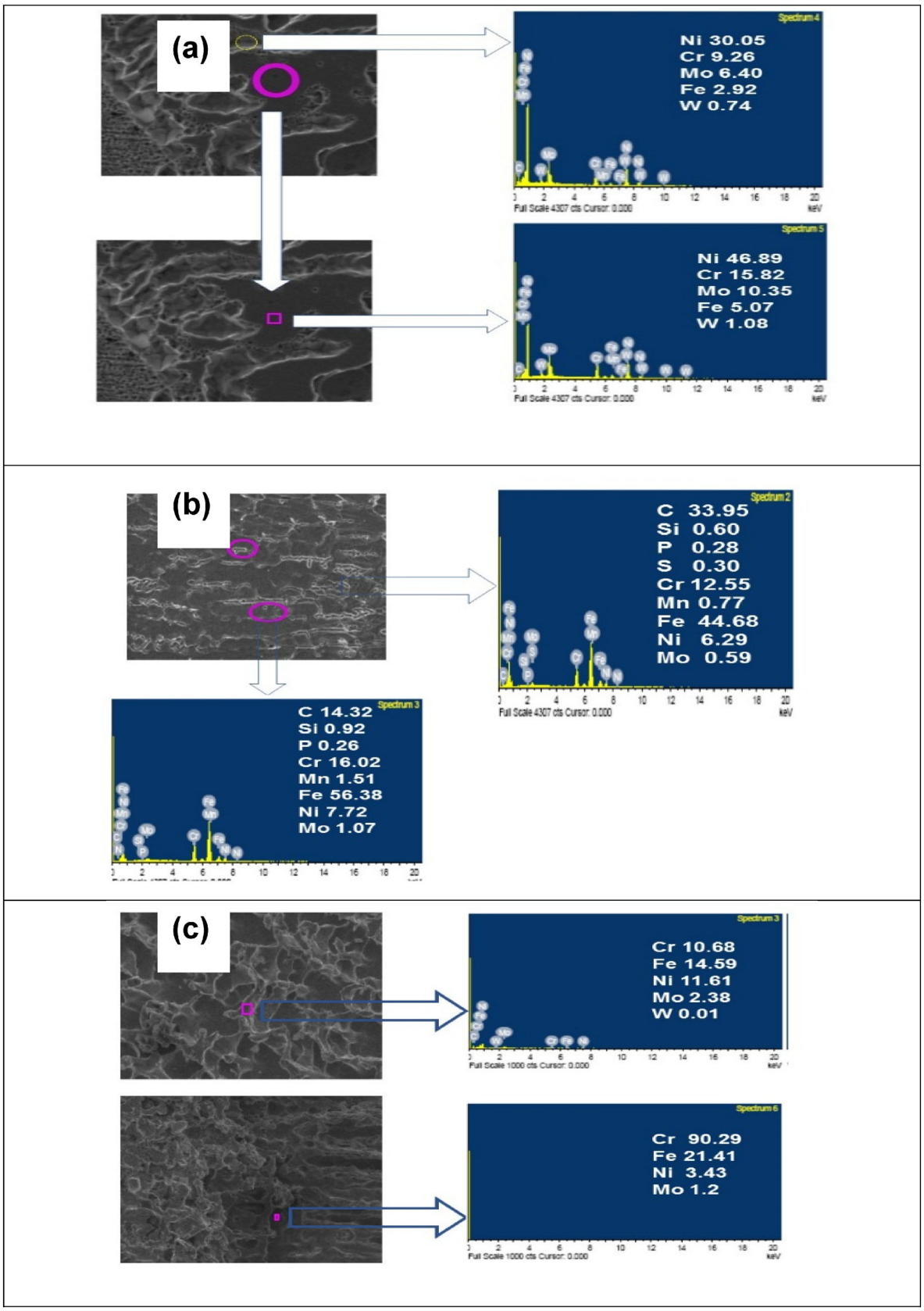

Fig.8 SEM/EDS image shows FZ of weld metals fabricated using CCGTAW process; (**a**) HAS C-276-HAS C-276; (**b**) SS 316 L-SS 316 L; (**c**) HAS C-276-SS 316 L

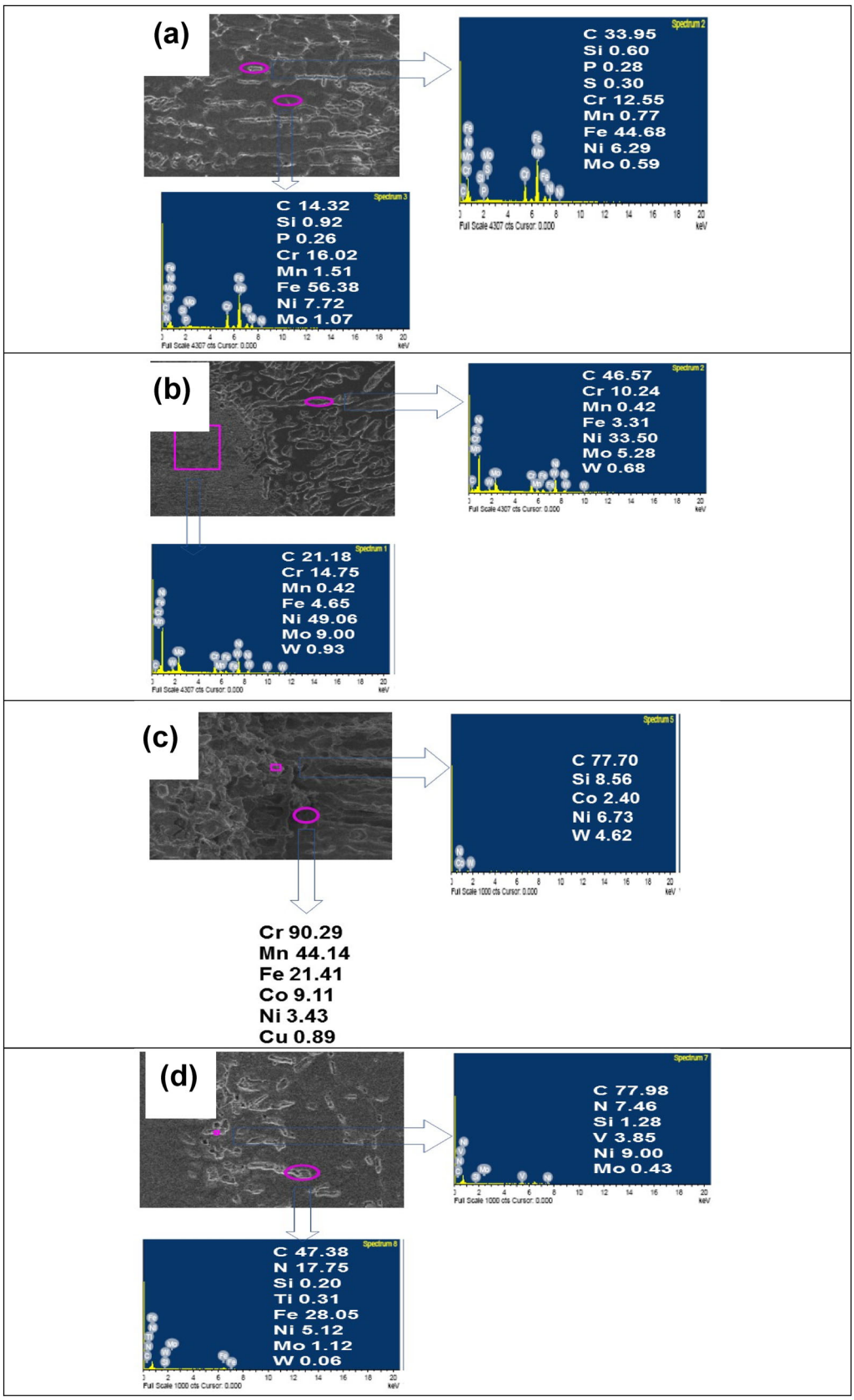

Fig.9 SEM/EDX image of IF region of weld metals fabricated using CCGTAW; (**a**) SS 316 L-SS 316 L; (**b**) HAS C-276-HAS C-276; (**c**) HAS C-276-SS 316 L (SS 316 L side); (**d**) HAS C-276-SS 316 L (HAS C-276 side)

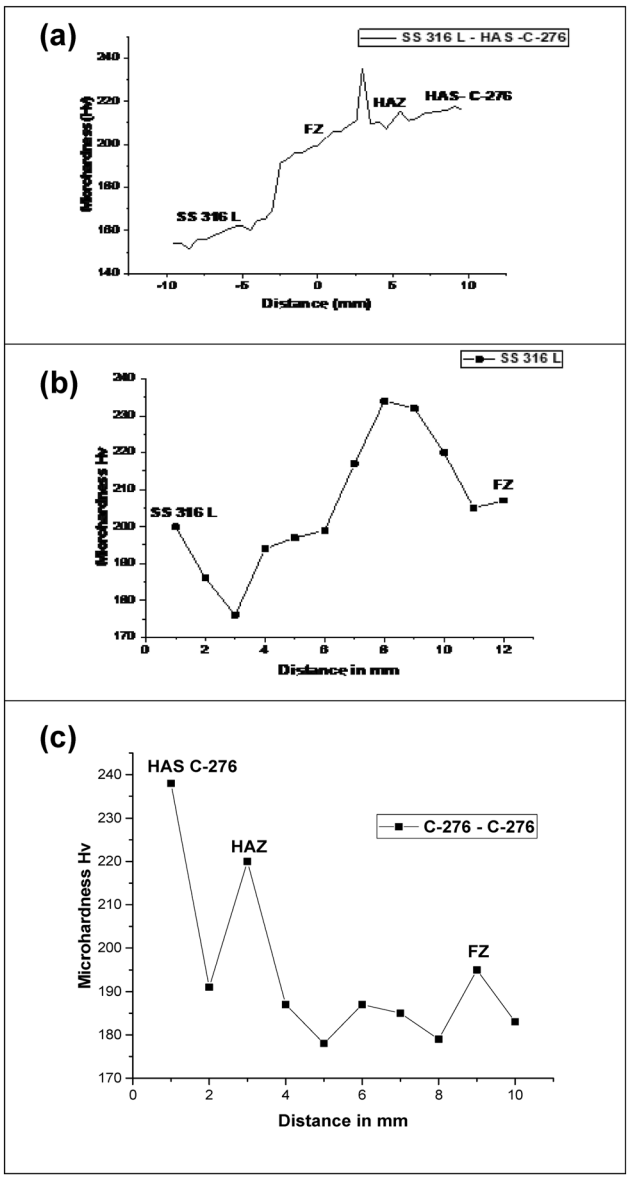

Fig.10 Microhardness graph of similar and dissimilar weldments fabricated using CCGTAW process

C-276 side, the microstructure reveals more uneven IF zone as compared to the SS 316 L side and moreover there is no any evidence of PMZ.

3.4 SEM/EDS Analysis

3.4.1 Fusion Zone

Figure 8c shows FZ microstructure of dissimilar welded joints. The welding process is composed of both the heating and cooling of the weldments, which greatly affects the mechanical properties of the weldments. Furthermore, GTAW process is associated with high heat input which results in segregations of alloying elements and formation of brittle tetragonal closed packed phases (TCP) phases named as sigma, P and μ [10]. From Fig. 8 SEM images, one can observe the presence of columnar dendritic and cellular structure in FZ of GTAW welded dissimilar joints. EDS point analysis was performed for the both similar and dissimilar welded joints to study the microsegregation formation in FZ. From EDS results, it is concluded that the subgrain boundary was enhanced with higher amount Mo, W and lower amount in Ni compared to subgrain body as shown in Fig. 8c. The EDS spectra clearly reveals that these phases were highly enhanced with Mo and W content and depleted in Ni and Fe content as depicted in Fig. 8c. Moreover, due to the high input with slow cooling rate of GTAW process, small amount of TCP phases was found in the microstructure. Therefore, this slow cooling rate triggers hot cracking in the weldments [3, 20, 21].

Figure 8a shows the FZ microstructure in similar HAS C-276-HAS C-276 welded joints. Figure 8a shows SEM/EDX image of FZ of GTAW weldments. As shown in Fig. 8a, in FZ, the subgrain boundaries are have higher Mo content and lower W content as compared to Mo, but lower in Ni compared to subgrain interiors. As compared to the similar (HAS C-276- Has C-276) and dissimilar (HAS C-276-SS 316 L) welded joints FZ, the enrichment of Mo is lesser in SS 316 L-SS 316 L similar welded joints, which is clearly shown in Fig. 8b.

3.4.2 Interface Area

Figure 9 shows the SEM/EDS analysis of the weld interface region of similar and dissimilar joints fabricated by GTAW process. Migrated grain boundaries (MGBs) were found at the weld interface region of SS 316 L side and Hastelloy C-276 side, respectively (See Fig. 9c and d). Since the joints were fabricated by GTAW process, the elemental segregation was more in between the subgrain body and subgrain boundary. This effect, clearly revealed by the EDS point analysis, is due to the higher heat input that associated with GTAW process. Furthermore, significant amount of TCP phases was also obtained at the weld interface region of Hastelloy C-276 side (See Fig. 9d). Moreover, these phases consisted of higher amount of Mo and depleted to a higher amount in Ni compared to FZ as shown in Fig. 9d (EDS image). Hence, it is concluded that as compared to FZ, the weld interface region was found to be more susceptible to hot cracking, and the same results have also been reported by Manikandan et al. [5]. As discussed previously, the subgrain boundary gets enriched with Mo content and has lower content Mo in the subgrain body in the similar HAS C-276-

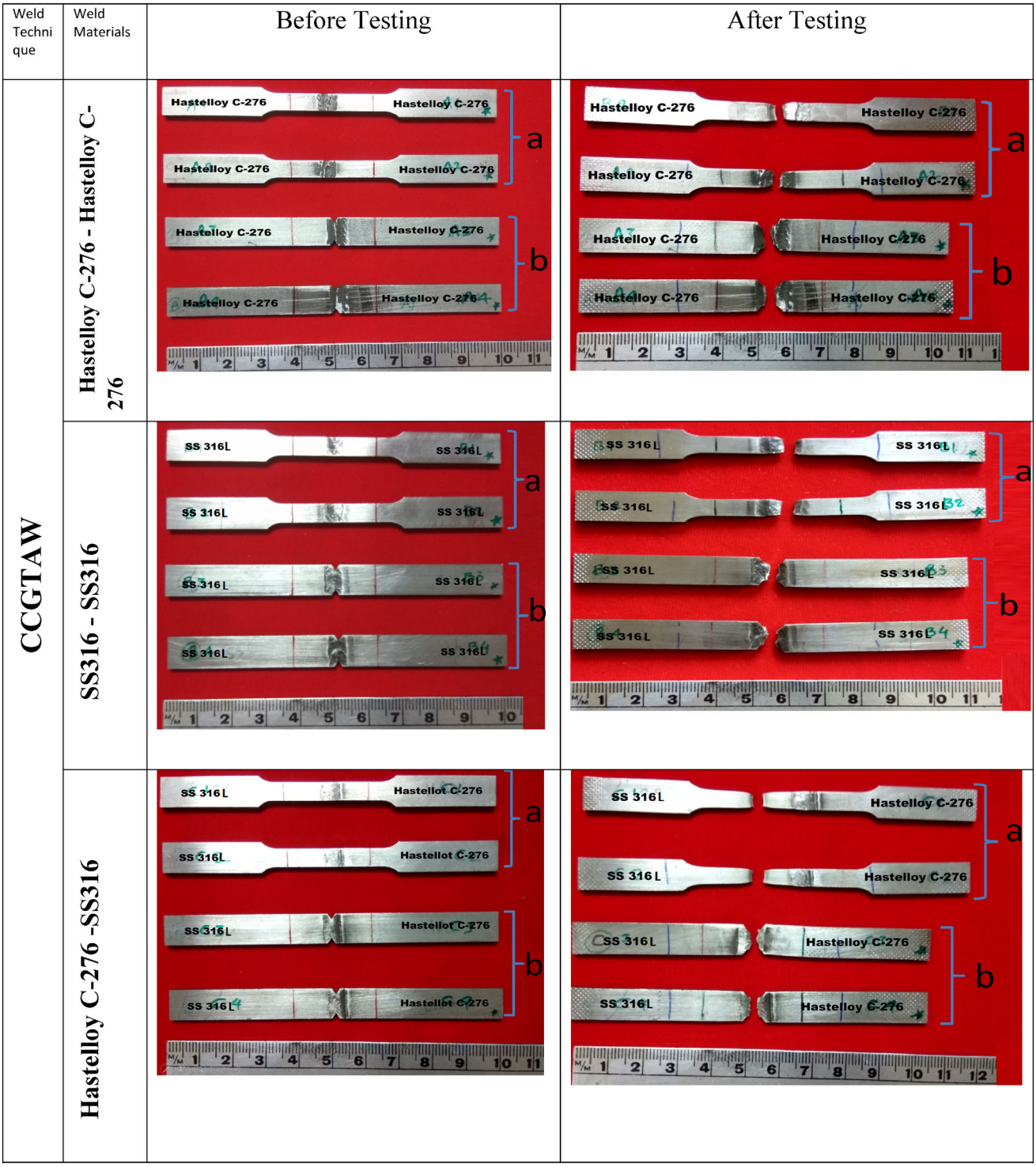

Fig.11 Photograph showing the CCGTAW weldments of Hastelloy C-276 and SS316 L (**a**) Tensile specimen (notched) and (**b**) Tensile specimen (unnotched)

HAS C-276 weld interface which is clearly shown in Fig. 9b. Considering the similar interface region for similar SS 316 L-SS 316 L joints, the lower content of Mo in subgrain boundary and rich Mo content are exhibited in the subgrain body, which is clearly shown in Fig. 9a.

Table 4 Tensile test of similar and dissimilar weld metals fabricated using CCGTAW process

Welding process	Material	Ultimate strength (MPa)	Notch tensile strength (MPa)	Joint efficiency (%)	Notch strength ratio (NSR)	Failure location
CCGTAW	HAS-HAS	740	796	98	1.07	FZ
	SS-SS	552	727	97	1.31	FZ
	HAS-SS	780	719	138	0.92	BM- SS Side

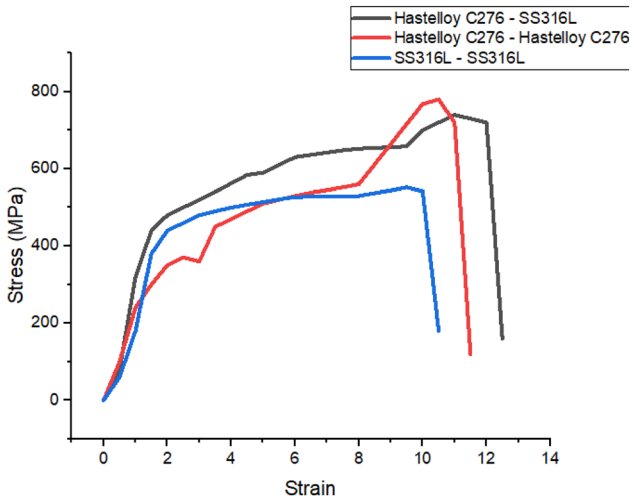

Fig.12 Stress–strain graph of HAS C-276 and SS-316 L joints made using CCGTAW process

4 Mechanical Characterization

4.1 Microhardness Test

The microhardness tests were conducted in the weld direction under GTAW conditions for similar welded joints of HAS-HAS, SS-SS, and dissimilar welded joints of HAS-SS. The hardness value increased when the plot moves from SS 316 side to the Hastelloy C-276 side (see Fig. 10a). The microhardness value of HAS C-276 was high as compared to the SS 316 L, this is due to the difference in chemical compositions of both the BMs [22]. The microhardness was reduced in FZ toward HAS C-276 side. This effect is due to rich Mo formation which tends to deplete other alloying elements in the matrix and may reduce hardness value [23]. Figure 10 shows that the unexpected change occurs in the microhardness value at the fusion zone boundary of the Hastelloy C-276. This may be due to the occurrence of PMZ area near to the FZ boundary. The microhardness of the similar welded joints was also evaluated for the comparison purposes as shown in Fig. 11. The microhardness value for the similar SS 316 L (see Fig. 10b) increased in trend up to the PMZ area, but sudden decrease was observed in hardness value, when the graph reaches the FZ area. Similar effect was observed for the similar HAS-C-276 (See Fig. 10C) welded joints using GTAW, as the hardness value decreases from the BM and sudden increase in hardness in the HAZ and FZ. It may be due to the intermetallic formation and larger grain size as compared to the BM area. However, the average microhardness for the dissimilar SS 316 L and HAS C-276 is 220 Hv. This microhardness value is higher as compared to the similar welded joints, SS 316 L and HAS C-276, i.e., 190 Hv and 210 Hv, respectively.

4.2 Tensile properties

UTS of the similar and dissimilar joints was obtained by the tensile testing. Figure 11 shows the tensile samples before and after tensile test of similar and dissimilar welded joints that are fabricated using GTAW. It was found that UTS of the dissimilar welded joints (HAS C-276-SS 316 L) was higher than the base metal, i.e., SS 316 L BM. Hence, the failure occurred in SS 316 L is away from the FZ of the weldments. The higher UTS was obtained for dissimilar (HAS C-276–SS 316 L) GTAW joints is 780 MPa compared to the similar welded joints of SS316 (552 MPa) and HAS C-276 (740). From Table 4, it can be seen that the UTS value of dissimilar (HAS C-276-SS 316 L) and similar (HAS-C-276) nearly same. This shows that the dissimilar joints welded using GTAW is effective and may be implemented in the boiler applications as discussed in the introduction. The tensile failure was situated for both similar weldments are in FZ. This shows that the dissimilar welded joints using GTAW of the HAS C-276-SS 316 L is effective and failure also occurred away from the FZ. The notch strength also exhibited a similar trend as followed by the welded samples in the tensile stress results. The study on notch effect of materials is of much significance for assessing the sensitivity of materials to notches, holes, grooves or other geometrical discontinuities [24]. Notch strength ratio (NSR) was calculated using results obtained between UTS of notched specimen and UTS of unnotched

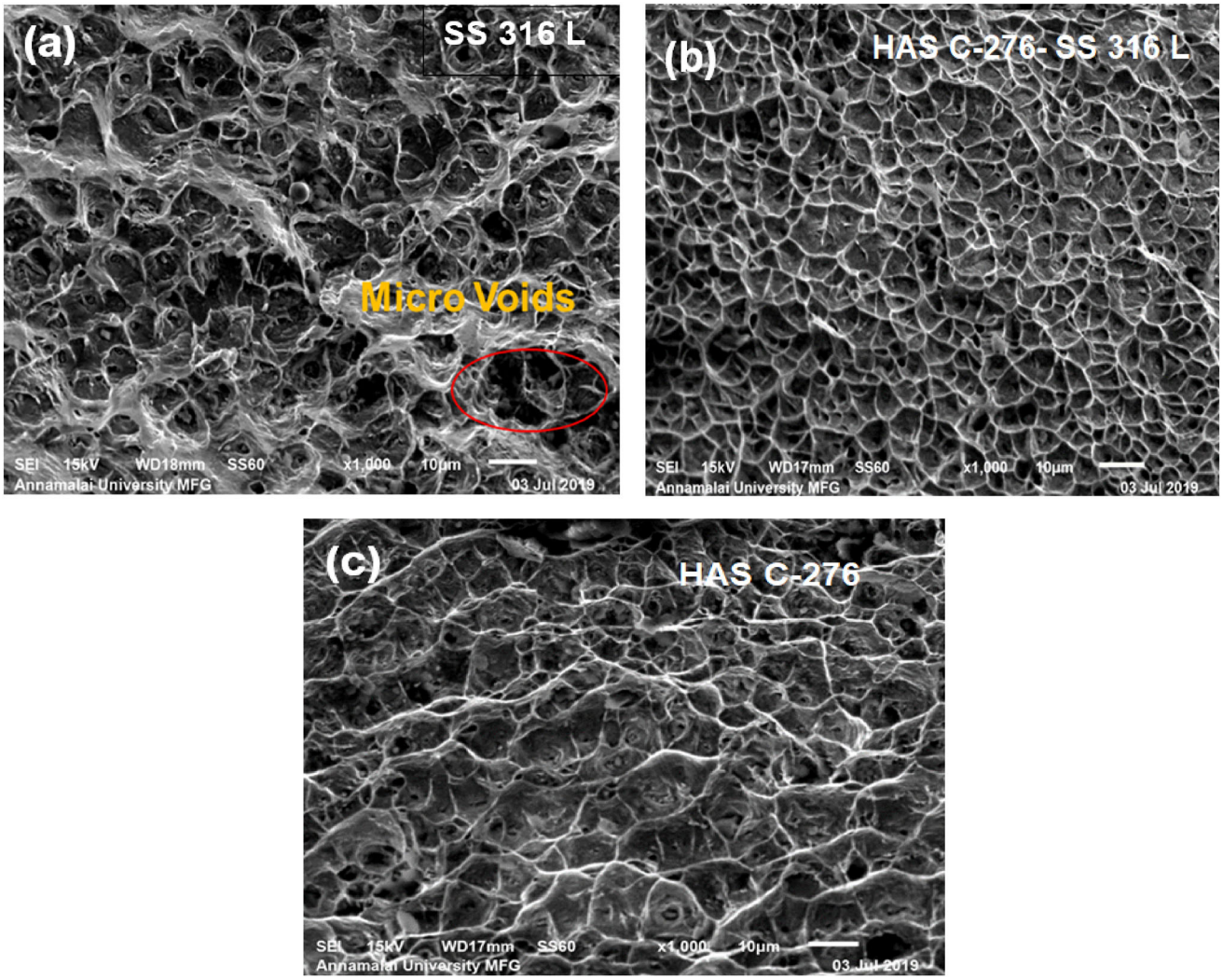

Fig.13 Fractography of similar and dissimilar welded metals fabricated using CCGTAW process

specimen. From Table 4 it can be inferred that dissimilar GTAW joints exhibit sensitivity to notches, and they come under the 'notch brittle materials' category. Of the three different combinations of similar and dissimilar welded joints, SS 316L-SS 316L joints result in the highest NSR of 1.31 (sensitivity to notches is lower) and dissimilar GTAW joints showed lowest NSR of 0.92 (sensitivity to notches is higher). NSR is higher than UTS that may be due to the larger plastic zone often results in more stress relaxations and finally an enhancement of nominal fracture stress and a larger NSR [25]. From Fig. 12, it is clearly evident that dissimilar combination of SS-HAS exhibited higher UTS as compared to the similar joints. The joint efficiency of the similar and dissimilar welded joints (SS316L-SS316L), (HAS C-276-HAS C-276) and (HAS C-276-SS316L) are 98, 97 and 138%, respectively.

The SEM micrographs of the fractured specimens showed a ductile mode of failure. This indicated microvoids and dimple appearance which appear to have gone through the plastic deformation for both the similar and dissimilar joints as shown in Fig. 13.

5 Conclusion

The SS 316 L and HAS C-276 base metals are welded using GTAW process. Three different variants of joints were fabricated, viz., SS 316 L-SS 316 L (similar), HAS C-276-HAS C- 276 (similar), and SS 316L-HAS C-276 (dissimilar). The welding conditions were optimized to obtain defect free joints and the weldments were characterized using OM, and SEM/EDS. Also, the weldments were tested using tensile test and hardness to find the mechanical properties of the joints. Based upon the investigation the following conclusions were drawn.

(i). Compared to the similar (HAS C-276- Has C-276) and dissimilar (HAS C-276-SS 316 L) welded joints FZ, the enrichment of Mo is lesser in SS 316 L-SS 316 L similar welded joints.

(ii). As compared to the similar joints, the dissimilar joints exhibit less grain coarsening that tends to achieve higher mechanical properties.

(iii). UTS of the dissimilar welded joints (HAS C-276-SS 316 L) was higher than the base metal, i.e., SS 316 L BM. Hence, the failure occurred in the SS 316 L is away from the FZ of the weldments.

(iv). The UTS obtained for dissimilar (HAS C-276-SS 316 L) GTAW joints is 780 MPa which is higher compared to the similar welded joints of SS316 (552 MPa) and HAS C-276 (740).

(v). The average microhardness for the dissimilar SS 316 L and HAS C-276 is 220 Hv, which is higher as compared to that of similar welded joints, SS 316 L and HAS C-276, i.e., 190 Hv and 210 Hv, respectively.

References

[1] Verma, J., Taiwade, R. V., Khatirkar, R. K., Sapate, S. G., & Gaikwad, A. D. (2017). Microstructure, mechanical and intergranular corrosion behavior of dissimilar DSS 2205 and ASS 316L shielded metal arc welds. *Transactions of the Indian Institute of Metals*, *70*(1), 225-237.

[2] Bhattacharyya, D., Davis, J., Drew, M., Harrison, R. P., & Edwards, L. (2015). Characterization of complex carbide–silicide precipitates in a Ni–Cr–Mo–Fe–Si alloy modified by welding. *Materials Characterization*, *105*, 118-128.

[3] Mousavi, S. A., & Sufizadeh, A. R. (2009). Metallurgical investigations of pulsed Nd: YAG laser welding of AISI 321 and AISI 630 stainless steels. *Materials & Design*, *30*(8), 3150-3157.

[4] Yılmaz, R., & Tümer, M. (2013). Microstructural studies and impact toughness of dissimilar weldments between AISI 316 L and AH36 steels by FCAW. *The International Journal of Advanced Manufacturing Technology*, *67*(5-8), 1433-1447.

[5] Manikandan, M., Arivazhagan, N., Rao, M. N., & Reddy, G. M. (2014). Microstructure and mechanical properties of alloy C-276 weldments fabricated by continuous and pulsed current gas tungsten arc welding techniques. *Journal of Manufacturing processes*, *16*(4), 563-572.

[6] Manikandan, M., Arivazhagan, N., Rao, M. N., & Reddy, G. M. (2015). Improvement of microstructure and mechanical behavior of gas tungsten arc weldments of alloy C-276 by current pulsing. *Acta Metallurgica Sinica (English Letters)*, *28*(2), 208-215.

[7] Rajkumar, V., & Arivazhagan, N. (2014). Role of pulsed current on metallurgical and mechanical properties of dissimilar metal gas tungsten arc welding of maraging steel to low alloy steel. *Materials & Design*, *63*, 69-82.

[8] Tariq, F., Baloch, R. A., Ahmed, B., & Naz, N. (2010). Investigation into microstructures of maraging steel 250 weldments and effect of post-weld heat treatments. *Journal of Materials Engineering and Performance*, *19*(2), 264-273.

[9] Dokme, F., Kulekci, M. K., & Esme, U. (2018). Microstructural and mechanical characterization of dissimilar metal welding of Inconel 625 and AISI 316L. *Metals*, *8*(10), 797.

[10] Sharma, S., Taiwade, R. V., & Vashishtha, H. (2017). Effect of continuous and pulsed current gas tungsten arc welding on dissimilar weldments between hastelloy C-276/AISI 321 austenitic stainless steel. *Journal of Materials Engineering and Performance*, *26*(3), 1146-1157.

[11] Pandit, S., Joshi, V., Agrawal, M., Manikandan, M., Ramkumar, K. D., Arivazhagan, N., & Narayanan, S. (2014). Investigations on mechanical and metallurgical properties of dissimilar continuous GTA welds of Monel 400 and C-276. *Procedia Engineering*, *75*, 61-65.

[12] Sharma, S., Taiwade, R. V., Vashishtha, H., & Mukherjee, S. (2018). Microstructural characterization, mechanical properties and corrosion behaviour of pulsed current GTA welded bimetallic joints between superalloy C-276 and stabilized austenitic stainless steel grade 321. *Materials Research Express*, *6*(1), 016532.

[13] Kumar, B. R. (2011). Weld quality analysis of TIG, laser and electron beam welded SS 304 and 316 materials with NDT techniques. In Proceedings of the National Seminar & Exhibition on Non-Destructive Evaluation NDE, Chennai (pp. 346–349).

[14] Radha Raman, T. A. (2004). A study of Tensile Strength of MIG and TIG welded dissimilar joints of mild steel and stainless steel. Mater SciEng A, 2004, 23-32.

[15] P. K. Taraphdar, C. Pandey, M. Mahapatra (2020). Finite element investigation of IGSCC-prone zone in AISI 304L multipass groove welds. Archives of Civil and Mechanical Engineering 20:54

[16] Pandeya Chandan, Mohan Mahapatrab M, Pradeep Kumara N (2018). Some studies on P91 steel and their weldments. Journal of Alloys and Compounds. 743. 332-364.

[17] Sirohia S, Pandey C, Goyala A. (2020) Characterization of structure-property relationship of martensitic P91 and high alloy ferritic austenitic F69 steel International Journal of Pressure Vessels and Piping. 188, 104179.

[18] Pandeya C, Mohan M, Pradeep Kumara N. (2017). Comparative study of autogenous tungsten inert gas welding and tungsten arc welding with filler wire for dissimilar P91 and P92 steel weld joint. Materials Science and Engineering: A. 712, 720-737.

[19] Malarvizhi, S., & Balasubramanian, V. (2012). Influences of welding processes and post-weld ageing treatment on mechanical and metallurgical properties of AA2219 aluminium alloy joints. *Welding in the World*, *56*(9-10), 105-119.

[20] Ming, H., Zhang, Z., Wang, J., Han, E. H., & Ke, W. (2014). Microstructural characterization of an SA508–309L/308L–316L domestic dissimilar metal welded safe-end joint. *Materials characterization*, *97*, 101-115.

[21] Cieslak, M. J., Headley, T. J., & Romig, A. D. (1986). The welding metallurgy of HASTELLOY alloys C-4, C-22, and C-276. *Metallurgical Transactions A*, *17*(11), 2035-2047.

[22] Hosseini, H. S., Shamanian, M., & Kermanpur, A. (2011). Characterization of microstructures and mechanical properties of Inconel 617/310 stainless steel dissimilar welds. *Materials characterization*, *62*(4), 425-431.

[23] Ramkumar, K. D., Dev, S., Saxena, V., Choudhary, A., Arivazhagan, N., & Narayanan, S. (2015). Effect of flux addition on the microstructure and tensile strength of dissimilar weldments involving Inconel 718 and AISI 416. *Materials & Design*, *87*, 663-674.

[24] Pandeya C, Mahapatrab M Pradeep Kumara N. (2018). Effect of strain rate and notch geometry on tensile properties and fracture mechanism of creep strength enhanced ferritic P91 steel. Journal of Nuclear Materials. 498, 176-186.

[25] Pandeya C, Mahapatra M. (2019). Role of evolving microstructure on the mechanical behaviour of P92 steel welded joint in as-welded and post weld heat treated state. 263: 241–55.